Gene cluster conservation provides insight into cercosporin biosynthesis and extends production to the genus *Colletotrichum*

Ronnie de Jonge[a,b,c,d,1,2], Malaika K. Ebert[e,f,g,1], Callie R. Huitt-Roehl[h,1], Paramita Pal[h], Jeffrey C. Suttle[e], Rebecca E. Spanner[e,f], Jonathan D. Neubauer[e], Wayne M. Jurick II[i], Karina A. Stott[e,f], Gary A. Secor[f], Bart P. H. J. Thomma[g], Yves Van de Peer[b,c,d,j], Craig A. Townsend[h,2], and Melvin D. Bolton[e,f,2]

[a]Plant-Microbe Interactions, Department of Biology, Science4Life, Utrecht University, 3584 CH, Utrecht, The Netherlands; [b]Department of Plant Biotechnology and Bioinformatics, Ghent University, B-9052, Ghent, Belgium; [c]VIB Center for Plant Systems Biology, B-9052 Ghent, Belgium; [d]Bioinformatics Institute Ghent, Ghent University, B-9052 Ghent, Belgium; [e]Red River Valley Agricultural Research Center, US Department of Agriculture, Fargo, ND 58102; [f]Department of Plant Pathology, North Dakota State University, Fargo, ND 58108; [g]Laboratory of Phytopathology, Wageningen University, 6708 PB Wageningen, The Netherlands; [h]Department of Chemistry, The Johns Hopkins University, Baltimore, MD 21218; [i]Food Quality Laboratory, US Department of Agriculture, Beltsville, MD 20705; and [j]Department of Genetics, Genomics Research Institute, University of Pretoria, 0028 Pretoria, South Africa

Edited by Paul Schulze-Lefert, Max Planck Institute for Plant Breeding Research, Cologne, Germany, and approved May 4, 2018 (received for review July 18, 2017)

Species in the genus *Cercospora* cause economically devastating diseases in sugar beet, maize, rice, soy bean, and other major food crops. Here, we sequenced the genome of the sugar beet pathogen *Cercospora beticola* and found it encodes 63 putative secondary metabolite gene clusters, including the cercosporin toxin biosynthesis (*CTB*) cluster. We show that the *CTB* gene cluster has experienced multiple duplications and horizontal transfers across a spectrum of plant pathogenic fungi, including the wide-host range *Colletotrichum* genus as well as the rice pathogen *Magnaporthe oryzae*. Although cercosporin biosynthesis has been thought to rely on an eight-gene *CTB* cluster, our phylogenomic analysis revealed gene collinearity adjacent to the established cluster in all *CTB* cluster-harboring species. We demonstrate that the *CTB* cluster is larger than previously recognized and includes cercosporin facilitator protein, previously shown to be involved with cercosporin autoresistance, and four additional genes required for cercosporin biosynthesis, including the final pathway enzymes that install the unusual cercosporin methylenedioxy bridge. Lastly, we demonstrate production of cercosporin by *Colletotrichum fioriniae*, the first known cercosporin producer within this agriculturally important genus. Thus, our results provide insight into the intricate evolution and biology of a toxin critical to agriculture and broaden the production of cercosporin to another fungal genus containing many plant pathogens of important crops worldwide.

natural product | perylenequinone | secondary metabolism | cercosporin | *Cercospora*

Among the most speciose genera in all of Fungi are the *Cercospora* (1). First described in 1863 (2), the genus has sustained a long history, largely due to notoriety as the causal agent of leaf spot diseases in a wide range of plants, including agriculturally important crops such as sugar beet, soybean, maize, and rice that together account for hundreds of millions of dollars in lost revenue annually to growers worldwide (3–8). Although *Cercospora* spp. share several characteristics associated with pathogenicity, such as penetration through natural openings and extracellular growth during the biotrophic stage of infection, most rely on the production of the secondary metabolite (SM) cercosporin (**1**) to facilitate infection (9, 10). Studies spanning nearly 60 y have made cercosporin a model perylenequinone (11), a class of SMs characterized by a core pentacyclic conjugated chromophore that gives rise to its photoactivity. When exposed to ambient light, cercosporin is a potent producer of reactive oxygen species in the presence of oxygen (12), with a quantum efficiency of >80% (13). This small molecule is lipophilic and can readily penetrate plant leaves, leading to indiscriminate cellular damage within minutes of exposure (14). Indeed, cercosporin is nearly universally toxic to a wide array of organisms, including bacteria, mammals, plants, and most fungal species, with the key exception of cercosporin-producing fungi, which exhibit cercosporin autoresistance. To date, cercosporin has been reported to be produced only by *Cercospora* spp., with the single exception of the brassica pathogen *Pseudocercosporella capsellae* (15). However, *Pseudocercosporella* and *Cercospora* are phylogenetically closely related, residing in a large clade within Mycosphaerellaceae (16).

In contrast to the large body of information on cercosporin biology spanning several decades (17, 18), the cercosporin toxin

Significance

Species in the fungal genus *Cercospora* cause diseases in many important crops worldwide. Their success as pathogens is largely due to the secretion of cercosporin during infection. We report that the cercosporin toxin biosynthesis (*CTB*) gene cluster is ancient and was horizontally transferred to diverse fungal plant pathogens. Because our analyses revealed genes adjacent to the established *CTB* cluster with similar evolutionary trajectories, we evaluated their role in *Cercospora beticola* to show that four are necessary for cercosporin biosynthesis. Lastly, we confirmed that the apple pathogen *Colletotrichum fioriniae* produces cercosporin, the first case outside the family Mycosphaerellaceae. Other *Colletotrichum* plant pathogens also harbor the *CTB* cluster, which points to a wider role that this toxin may play in virulence.

Author contributions: R.d.J., C.R.H.-R., C.A.T., and M.D.B. designed research; R.d.J., M.K.E., C.R.H.-R., P.P., J.C.S., R.E.S., J.D.N., W.M.J., and K.A.S. performed research; G.A.S., B.P.H.J.T., Y.V.d.P., C.A.T., and M.D.B. contributed new reagents/analytic tools; R.d.J., M.K.E., C.R.H.-R., P.P., J.C.S., C.A.T., and M.D.B. analyzed data; and R.d.J., M.K.E., C.R.H.-R., C.A.T., and M.D.B. wrote the paper.

The authors declare no conflict of interest.

This article is a PNAS Direct Submission.

Data deposition: The sequences reported in this paper have been deposited in the National Center for Biotechnology Information, https://www.ncbi.nlm.nih.gov/bioproject/PRJNA270309 (BioProject ID: PRJNA270309). Custom code and auxillary data are available through Zenodo (https://doi.org/10.5281/zenodo.1156551) and Figshare (http://doi.org/10.6084/m9.figshare.4056522), respectively.

[1]R.d.J., M.K.E., and C.R.H.-R. contributed equally to this work.

[2]To whom correspondence may be addressed. Email: r.dejonge@uu.nl, ctownsend@jhu.edu, or melvin.bolton@ars.usda.gov.

This article contains supporting information online at www.pnas.org/lookup/suppl/doi:10.1073/pnas.1712798115/-/DCSupplemental.

Published online May 29, 2018.

biosynthesis (*CTB*) gene cluster was only recently resolved in *Cercospora nicotianae* (19). The keystone enzyme for cercosporin biosynthesis, CTB1, bears all the hallmarks of an iterative, nonreducing polyketide synthase (PKS) (20). Using *CTB1* as a point of reference, the complete *C. nicotianae CTB* gene cluster was determined to consist of eight contiguous genes, of which six are believed to be responsible for cercosporin assembly (*CTB1*, *2*, *3*, *5*, *6*, and *7*) (19, 21). The zinc finger transcription factor CTB8 coregulates expression of the cluster (19), while the major facilitator superfamily transporter CTB4 exports the final metabolite (22). Downstream of the *CTB* cluster are two ORFs encoding truncated transcription factors, while loci designated as *ORF9* and *ORF10* upstream of the *CTB* cluster are not regulated by light and are not believed to encode proteins with metabolic functions (19). Consequently, the clustering of eight genes with demonstrated coregulation by light that are flanked by ORFs with no apparent role in cercosporin biosynthesis has suggested that cercosporin production relies on the eight-gene *CTB* cluster (19). In this study, we used an evolutionary comparative genomics approach to show that the *CTB* gene cluster underwent multiple duplication events and was transferred horizontally across large taxonomic distances. Since these horizontal transfer events included genes adjacent to the canonical eight-gene *CTB* cluster, we used reverse genetics to show that the *CTB* cluster includes additional genes in *Cercospora beticola*, including one gene that was previously shown to be involved with cercosporin autoresistance (23) and four previously unrecognized genes involved with biosynthesis. The *CTB* cluster was found in several *Colletotrichum* spp., and we confirmed that the apple pathogen *Colletotrichum fioriniae* can also produce cercosporin. As all earlier understanding of cercosporin biosynthesis has been unwittingly limited by a truncated set of genes in *Cercospora* spp., the full dimension of the gene cluster provides deeper insight into the evolution, biosynthesis, and dissemination of a fungal toxin critical to worldwide agriculture.

Results

SM Cluster Expansion in *C. beticola*. *C. beticola* strain 09-40 was sequenced to 100-fold coverage and scaffolded with optical and genome maps, resulting in 96.5% of the 37.06-Mbp assembly being placed in 12 supercontigs, of which 10 are assumed to be chromosomes. Despite their ubiquitous presence in nature and cropping systems, genome sequences of *Cercospora* spp. are not well represented in public databases. Therefore, to aid comparative analysis within the *Cercospora* genus, we also sequenced the genome of *Cercospora berteroae* and reassembled the genome of *Cercospora canescens* (24) (*SI Appendix*, Table S1). To identify gene clusters responsible for biosynthesis of aromatic polyketides in *C. beticola*, we mined the genome to identify all SM clusters (25) and compared these with predicted clusters in related Dothideomycetes. The *C. beticola* genome possesses a total of 63 predicted SM clusters of several classes, representing an expanded SM repertoire with almost twice the number as compared with closely related Dothideomycetes fungi, which average 34 SM clusters (*SI Appendix*, Table S2 and Dataset S1). Notably, *C. beticola* encodes 23 candidate nonribosomal peptide synthetase clusters, which is considerably higher than most Dothideomycetes fungi, which have an average of 13 (26). To identify the *C. beticola* PKS cluster responsible for cercosporin biosynthesis, we compared the sequence of the *C. nicotianae CTB* cluster (19) with predicted PKS clusters of *C. beticola.* To fill in sequencing gaps between genes in the *C. nicotianae CTB* cluster, we sequenced the genome of *C. nicotianae*, which showed that *C. beticola* PKS *CBET3_00833* (*CbCTB1*) and flanking genes (*CBET3_00830* – *CBET3_00837*) were ∼96% identical to *C. nicotianae CTB1* to *CTB8*, and all genes were collinear, strongly suggesting that this region houses the *CTB* cluster in *C. beticola* (*SI Appendix*, Fig. S1).

Repeated Duplication and Lateral Transfer of the Cercosporin Biosynthetic Cluster. To study the evolutionary relationships of *C. beticola* PKSs, we conducted large-scale phylogenomic analyses that included various previously characterized PKSs from selected species (27). Because resolving orthologous relationships among PKSs can predict the type of SM that will be synthesized, we first built a phylogenetic tree of the conserved core β-ketoacyl synthase domains of each PKS that resulted in separating PKS enzymes into four major groups (*SI Appendix*, Fig. S2*A*). Among the eight *C. beticola* nonreducing PKSs, phylogenetic analysis revealed significant similarity among *Cb*CTB1, *CBET3_10910-RA*, and *CBET3_11350-RA*, which cluster at the base of the cercosporin clade (*SI Appendix*, Fig. S2*B*). Interestingly, genes flanking *CBET3_10910-RA*, but not *CBET3_11350-RA*, were also strikingly similar to *CbCTB* cluster genes (Fig. 1). Consequently, we hypothesized that the *CBET3_10910* SM cluster is the result of a *CTB* cluster duplication. Since duplicated SM gene clusters appeared to be relatively rare in fungi (28), we investigated the origin and specificity of the *CTB* cluster and the putative duplication by searching for *Cb*CTB1 homologs against a selected set of 48 published Ascomycetes proteomes (*SI Appendix*, Table S3) representing a diverse group of fungal orders. We identified *Cb*CTB1 orthologs in the *Cercospora* spp. *C. berteroae* and *C. canescens* and confirmed its presence in *Cladosporium fulvum* (27) and *Parastagonospora nodorum* (29). Surprisingly, seven additional orthologs were identified in Sordariomycetes species (*Colletotrichum orbiculare*, *Colletotrichum gloeosporioides*, *C. fioriniae*, *Colletotrichum graminicola*, *Colletotrichum higginsianum*, and *Magnaporthe oryzae*), as well as one within Leotiomycetes (*Sclerotinia sclerotiorum*) (*SI Appendix*, Fig. S3*A*), representing diverse taxa harboring *CTB1*. Analysis of sequence identity showed that intraspecies (*Cb*CTB1 to CBET3_10910-RA) sequence identity (45%) was lower than the interspecies [e.g., *Cb*CTB1 and *C. fulvum* CTB1 (Clafu1_196875)] sequence identity (55%) (*SI Appendix*, Table S4), suggesting that the *CTB1* duplication event occurred before Dothideomycetes speciation.

To develop a "phylogenetic roadmap" that may explain *CTB1* evolution, we used the process of "reconciliation" that takes into account both species and gene histories (30). Although not conclusive, reconciliation considers the costs of evolutionary events (i.e., gene duplications, transfers, and/or losses) to explain the most parsimonious evolutionary route to the present scenario (31). Reconciliation of the species tree (*SI Appendix*, Fig. S4) with the CTB1 protein tree revealed that the predicted evolutionary history of *CTB1* can be characterized by four duplications, three

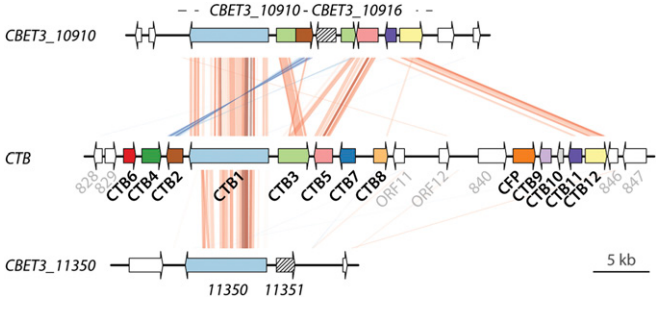

Fig. 1. The cercosporin biosynthetic cluster is duplicated and maintained in *C. beticola*. *CBET3_10910* and flanking genes are syntenic with the *CTB* cluster (*CBET3_00833* and flanking genes) in *C. beticola*. Alignment lines correspond to DNA fragments exhibiting significant similarity when the genomic regions comprising the gene clusters are compared with tBLASTx. Direct hits are displayed in red, whereas complementary hits are in blue. The intensity of the alignments represents the percentage similarity ranging from 23 to 100%. Genes flanking *CBET3_11350-RA* were not syntenic with *CTB* cluster genes.

transfers, and widespread loss to most species analyzed (*SI Appendix*, Fig. S5*A*) and further corroborates our hypothesis that the *CTB1* duplication event (D1) occurred early in Dothideomycetes speciation. Reconciliation also revealed an ancient *CTB1* ortholog in *S. sclerotiorum* (*SI Appendix*, Fig. S5*A*), suggesting that *CTB1* arose before speciation of Dothideomycetes. Duplications D2 to D4 arose after lateral transfer (T1) of *CTB1* into the last common ancestor of Glomerellales. *CTB1* was then transferred (T2) from a common ancestor in Glomerellales to *M. oryzae* (*SI Appendix*, Fig. S5*A*).

We extended the search for CTB cluster protein orthologs by scanning the 48 proteomes for homologs of *Cb*CTB2 (CBET3_00830) to *Cb*CTB8 (CBET3_00837), followed by phylogenetic tree construction and subtree selection (*SI Appendix*, Fig. S3 *B–N*). This resulted in the identification of orthologs in the same set of species previously listed to contain *CTB1*, with the only exceptions in cases where *CTB* gene homologs were lost in a species. Although the loss of *CTB6* and *CTB7* orthologs limits reconciliation analysis of these gene families, reconciliation of the subtrees for *CTB2*, *CTB3*, *CTB4*, *CTB5*, and *CTB8* (*SI Appendix*, Fig. S5 *B–H*) supported a similar scenario as proposed for *CTB1*, involving at least two duplications (D1 and D2) and two horizontal transfer events (T1 and T2) that explain the present-day *CTB* scenario (Fig. 2). However, an alternative explanation involving a single transfer to an ancestral Glomerellales species followed by widespread loss in most species in this lineage, except for *M. oryzae* and the analyzed *Colletotrichum* spp. (Fig. 2 and *SI Appendix*, Table S5), cannot be ruled out by our analyses at this stage.

Extension of the Predicted Cercosporin Biosynthetic Cluster Based on Microsynteny. To further examine the *CTB* clusters across all recipient species, we generated pairwise alignments relative to the *C. beticola CTB* cluster and flanks. To our surprise, we observed a striking level of similarity outside the known eight *CTB* genes on the 3′ end of the cluster (Fig. 3) in all *CTB*-containing genomes. To investigate whether the amount of microsynteny observed for the *CTB* cluster and these flanking genes can be reasonably expected when comparing Dothideomycetes and Sordariomycetes genomes, we assessed the genome-wide microsynteny between the genomes of *C. beticola* and *C. gloeosporioides* and between *C. beticola* and *M. oryzae*. This analysis identified the *CTB* cluster together with its flanking genes as having the highest level of microsynteny among all regions in the genome between *C. beticola* and *C. gloeosporioides* and showed that the observed *CTB* microsynteny between *C. beticola* and *M. oryzae* was also higher than the genome-wide average (Fig. 4). Likewise, sequence identity of most CTB proteins between *C. beticola* and *Colletotrichum* spp., and to a lesser degree with *M. oryzae*, is higher compared with the genome-wide average (*SI Appendix*, Figs. S6 and S7). In contrast, sequence conservation of CTB8, a Zn_2Cys_6 transcription factor previously implicated for transcriptional regulation of the *CTB* cluster (19), appears much lower than that of other CTB and non-CTB proteins and, therefore, is suggestive of positive diversifying selection. Considering the level of microsynteny and protein conservation, we hypothesized that these flanking genes are part of the *C. beticola CTB* cluster. To test this proposal, we first determined the relative expression of all eight established *C. beticola CTB* genes as well as a number of flanking genes (*CBET3_00828* to *CBET3_00848*) under light (cercosporin-inducing) vs. dark (cercosporin-repressing) conditions, which showed that all candidate *CTB* genes on the 3′ flank were induced in the light, except *CBET3_00846* and *CBET3_00848* (*SI Appendix*, Table S7). Functional annotation of these genes revealed one nonconserved phenylalanine ammonia lyase (CBET3_00840), the cercosporin facilitator protein (CFP) (23) (CBET3_00841), a candidate α-ketoglutarate–dependent dioxygenase (CBET3_00842), a dehydratase (CBET3_00843), a

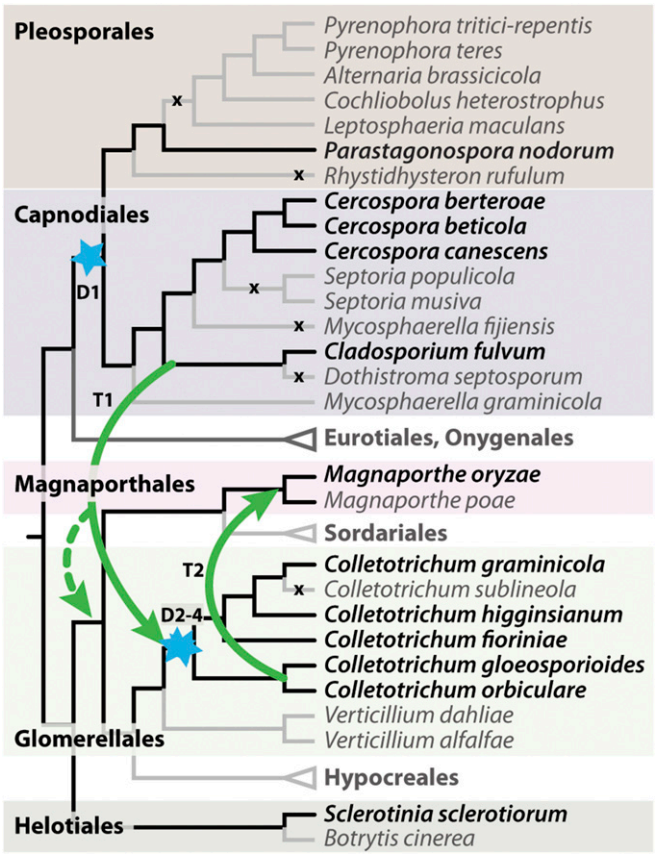

Fig. 2. Phylogenetic roadmap of *CTB* cluster evolution. Phylogenetic roadmap detailing the proposed evolutionary trajectory of the *CTB* cluster involving horizontal gene transfer events from Capnodiales to Glomerellales (T1) and another from Glomerellales to Magnaporthales (T2), as well as multiple duplications (D1 to D4) and frequent gene loss (x). Cladogram of the phylogenetic relationship of *Cercospora* spp. and 45 other sequenced fungi. The unscaled tree was constructed using CVTree. Duplication nodes are marked with blue stars, losses are indicated by x's, and transfers are highlighted by green arrows. Species without the *CTB* cluster are depicted in gray; those encompassing it are in black. An alternative and slightly less parsimonious scenario involving a single transfer from Capnodiales into the last common ancestor of Magnaporthales and Glomerellales is shown by the dashed arrow.

β-ig-h3 fasciclin (CBET3_00844), a laccase (CBET3_00845), zinc finger domain-containing protein (CBET3_00846), and protein phosphatase 2A (CBET3_00847; *SI Appendix*, Table S7), several of which have functions associated with multidomain enzymes or polyketide biosynthesis in fungi or bacteria (19, 22, 32–36). Phylogenetic analyses of these flanking genes and reconciliation of their respective protein phylogenies (*SI Appendix*, Figs. S3 and S5) with the species tree (*SI Appendix*, Fig. S4) suggest that all genes except *CBET3_00840*, *CBET3_00846*, and *CBET3_00847* have undergone highly similar evolutionary trajectories as the established *CTB* cluster genes (Fig. 2 and *SI Appendix*, Fig. S5), suggesting that the *CTB* cluster was transferred as a whole at least once, followed by species-specific evolutionary trajectories involving frequent gene loss as well as gene gain (Fig. 2). We further evaluated the hypothesis of horizontal cluster transfer using a comparative topology test that examines whether the determined tree topologies that support horizontal cluster transfer are significantly better than constrained topologies that would not support transfer. Tree topologies were compared using the Approximately Unbiased test (37), implemented in CONSEL (38) as previously described by Wisecaver and Rokas (39).

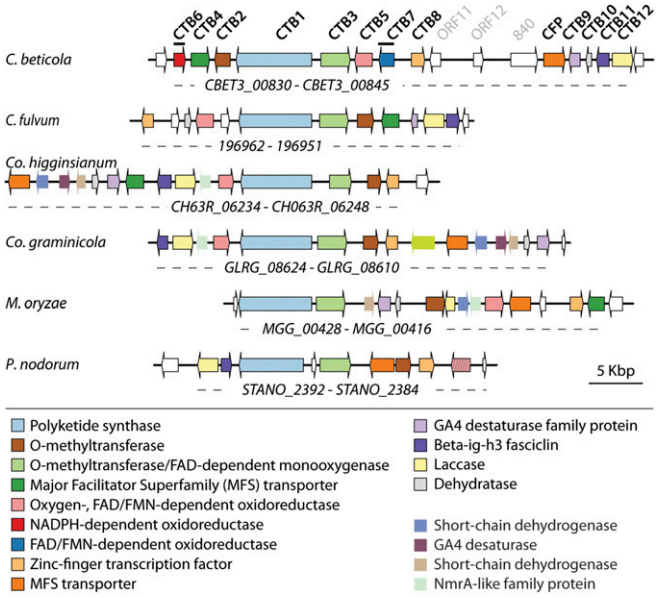

Fig. 3. Synteny and rearrangements of the conserved *C. beticola* cercosporin biosynthetic cluster. The cercosporin biosynthetic cluster in *C. beticola* (top line) and flanking genes are conserved in *C. fulvum*, *C. higginsianum*, *C. graminicola*, *M. oryzae*, and *P. nodorum*. For all species, the displayed identifiers are transcript IDs, and the corresponding sequences can be retrieved from JGI MycoCosm or ORCAE. *CTB* orthologs are colored relative to the *C. beticola CTB* cluster genes; the color key and annotated functions are highlighted below the *CTB* cluster graphic. *Cercospora*-specific *CTB* genes *CTB6* and *CTB7* are underlined.

Constrained topologies in which we force either a monophyletic origin of all Dothideomycetes proteins or a monophyletic origin of all Sordariomycetes proteins were significantly worse than trees without such constraint (*SI Appendix*, Table S6). Thus, the comparative topology tests support the previously determined topologies, which suggest horizontal cluster transfer.

***CTB* Genes Essential for Cercosporin Biosynthesis.** To confirm individual gene contributions for cercosporin production, we generated single-gene deletion mutants of all candidate genes from *CBET3_00840* to *CBET3_00846* and tested their ability to produce cercosporin. Initial assays of selected mutants showed that cercosporin production in Δ*CBET3_00844* and Δ*CBET3_00845* mutants was abolished, while Δ*CBET3_00842* mutants accumulated only a red, cercosporin-like metabolite that migrated differently in potato dextrose agar (PDA) culture plates and TLC (*SI Appendix*, Fig. S8). To provide more definitive analyses of cercosporin production, HPLC profiles were obtained from all candidate *CTB* gene mutants and compared with WT cercosporin (Fig. 5*A*). Unlike other analyzed mutants, Δ*CBET3_00840* and Δ*CBET3_00846* produced compounds with HPLC profiles like cercosporin (Fig. 5*A*), suggesting that these genes are not involved with cercosporin biosynthesis. Together, these results corroborate our hypothesis that the *CTB* cluster extends to at least *CBET3_00845* at the 3′ side and includes four additional *CTB* biosynthetic genes, as well as *CbCFP*. Consequently, we propose naming genes *CBET3_00842*, *CBET3_00843*, *CBET3_00844*, and *CBET_00845* as *CTB9* to *CTB12*, respectively (*SI Appendix*, Table S7).

Precercosporin Isolation and Characterization. To characterize the red metabolite that accumulated in the Δ*842/CTB9* and Δ*843/CTB10* mutants (Fig. 5*A* and *SI Appendix*, Fig. S8), an ethyl acetate extract of the collected mycelia was analyzed by reverse-phase HPLC. At 280 nm, a single peak was observed in both mutant extracts with identical retention times and UV-Vis spectra (Fig. 5). This peak was compared with a reference sample of cercosporin produced by wild-type *C. beticola*. The retention time of this peak was shorter than that of cercosporin, suggesting a more polar metabolite. Comparison of the UV-Vis spectra (Fig. 5 *B–D*) of the unknown compound and cercosporin revealed nearly identical chromophores, suggesting close structural relation. The exact mass of the metabolite from the mutants was determined (Δ*842/CTB9*: *m/z* 537.1762, Δ*843/CTB10*: *m/z* 537.1757, $[M+H^+]$), consistent with the elemental composition $C_{29}H_{28}O_{10}$. This mass is 2 Da greater than that of cercosporin (+2 hydrogens), which led to a proposed structure for precercosporin (**2**) (Fig. 6). Alternative hydroquinones of cercosporin could be excluded simply on the basis of the UV-Vis spectral information and chemical instability. The presence of a free phenol in precercosporin in place of the unusual seven-membered methylenedioxy of cercosporin is consonant with the red shift of the long wavelength (λ_{max}) and the shorter HPLC retention time.

To firmly support the tentative structure of precercosporin, the crude extract of Δ*842/CTB9* was further purified by reverse-phase HPLC. To obtain sufficient material for ^{1}H-NMR analysis, extractions were performed quickly and in low light and reduced temperature to slow apparent polymerization of precercosporin. The relative instability of precercosporin compared with cercosporin suggests a possible role for the methylenedioxy bridge in overall stability. Immediately evident from the ^{1}H-NMR spectrum (*SI Appendix*, Fig. S9*A*), apart from its overall similarity to that of cercosporin itself, was not only the absence of the methylenedioxy singlet at δ5.74 diagnostic of cercosporin but also the appearance of a new methoxyl signal at δ4.28 and a phenol at δ9.25. Consistent with the new asymmetry in precercosporin, two strongly hydrogen-bonded *peri*-hydroxy groups could be seen far downfield at around 15 ppm, and two aryl hydrogens were observed at δ6.92 and δ6.87. That these latter resonances are observed only in pairs (as are the two side-chain methyl doublets at around 0.6 ppm) and the other signals are doubled implies that precercosporin is formed as a single atropisomer having a helical configuration likely identical to that of cercosporin, although it is conceivable that CTB9 or CTB10 sets the final stereochemistry.

^{13}C-NMR spectroscopy data were obtained by growing a larger number of PDA plates of Δ*842/CTB9* supplemented with 2 mM [1-^{13}C]-sodium acetate and 2 mM [2-^{13}C]-sodium acetate to equally enrich all polyketide-derived carbons (~3% per site). Working quickly to isolate and purify precercosporin in low light and low temperature as described earlier, both 1D and heteronuclear single quantum coherence spectra of precercosporin were acquired (*SI Appendix*, Fig. S9 *B* and *C*). As seen in the ^{1}H-NMR spectrum, breaking the symmetry of cercosporin was evident in the observation of all 29 carbons in the ^{13}C-NMR

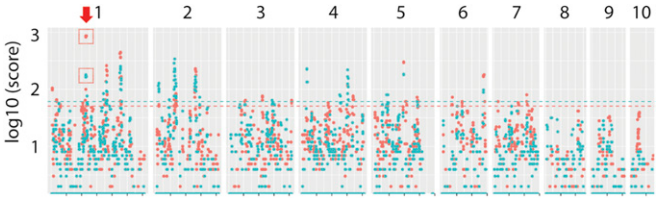

Fig. 4. *CTB* cluster microsynteny conservation segregates from the genome-wide average. The genome-wide, gene-by-gene microsynteny between *C. beticola* and *C. gloeosporioides* (depicted in red) and between *C. beticola* and *M. oryzae* (in blue) across the 10 assembled *C. beticola* chromosomes is shown. Each dot represents one *C. beticola* gene and its respective microsynteny score. The red arrow indicates the position of the *CTB* cluster on chromosome 1 and coincides with high microsynteny in both *C. gloeosporioides* and *M. oryzae*. The dashed lines represent the 99th quantile of the microsynteny scores for both comparisons independently.

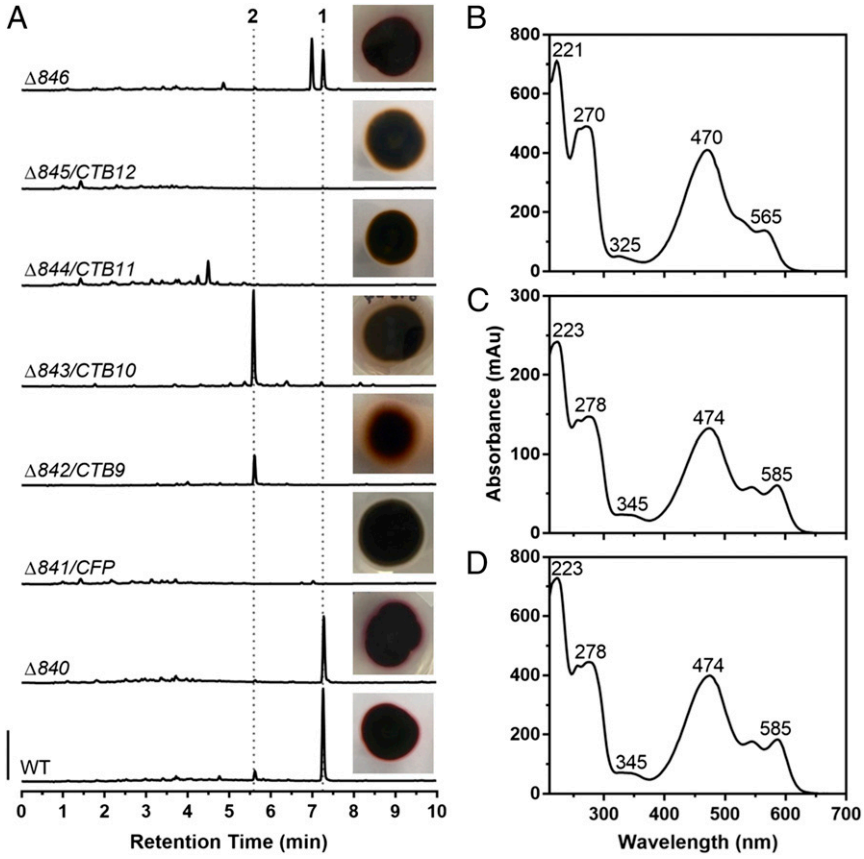

Fig. 5. Analysis of cercosporin production in *CTB* mutants of *C. beticola*. Site-directed knockout mutants in genes *CBET3_00840*, *CFP (CBET3_00841)*, *CTB9* (*CBET3_00842*), *CTB10* (*CBET3_00843*), *CTB11* (*CBET3_00844*), *CTB12* (*CBET3_00845*), and *CBET3_00846* were assayed for cercosporin production by HPLC. Cercosporin extracted from *C. beticola* strain 10-73-4 (WT) was used as a positive control. (*A*) 280 nm HPLC chromatograms and images of representative colonies for each knockout. (Scale bar, 250 mAu.) Cercosporin (**1**) and precercosporin (**2**) peaks are indicated by dashed lines. (*B–D*) UV-Vis spectra from wild-type *C. beticola* (7.25-min peak in *B*), *C. beticola* Δ*CTB9* (5.36-min peak in *C*), and *C. beticola* Δ*CTB10* (5.36-min peak in *D*) were extracted from 280 nm HPLC chromatograms. Wavelengths of relevant UV maxima are indicated.

spectrum, which notably revealed three methoxyl groups and diagnostic doubling of all resonances, save two overlapping pairs of signals. This behavior is fully in accord with the assigned structure of precercosporin.

Identification of Cercosporin from *C. fioriniae*. Because our initial phylogenomic analyses suggested that several *Colletotrichum* spp. harbored *CTB* clusters (Figs. 2 and 3), we questioned whether the *CTB* cluster can be found in additional *Colletotrichum* spp. CTB protein orthology analysis revealed that 8 of the 13 *Colletotrichum* spp. hosted at Ensembl Fungi (https://fungi.ensembl.org/index.html) encode a similar set of CTB proteins as observed in *C. higginsianum* (*SI Appendix*, Table S8). These eight species are plant pathogens of crops such as apple, safflower, melon, and cucumber; a variety of *Brassica* and cereal crops; as well as various tree species (40–46) (*SI Appendix*, Figs. S10 and S11 and Table S8). Remarkably, many species have lost several *CTB* genes, such as the endophyte *Colletotrichum tofieldiae*, which has lost the cluster entirely (*SI Appendix*, Figs. S10 and S11 and Table S8).

Earlier reports suggested the production of a red pigment by some *Colletotrichum* spp. such as the apple pathogen *C. fioriniae* (47, 48); therefore, we questioned whether the red pigment was cercosporin. As a first step, two *C. fioriniae* strains (HC89 and HC91) from our collection that were previously isolated from apple were assayed for cercosporin production using the KOH assay (49). No cercosporinlike pigment was observed in the medium under the same conditions that stimulate cercosporin production in *C. beticola*. Since epigenetic modifiers have been used to induce production of SMs in fungal species (50, 51), we considered whether this strategy could be used to induce cercosporin production in *C. fioriniae*. Medium augmented with the histone deacetylase inhibitor trichostatin A (TSA) (50) induced

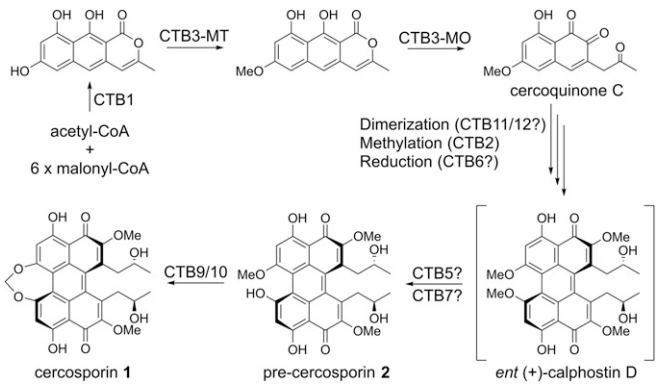

Fig. 6. Proposed biogenesis of cercosporin. Tentative proposal for biosynthesis of cercosporin (**1**), incorporating biosynthetic genes identified in this study. Intermediates in brackets are logically inferred and have not been directly observed. MO, monooxygenase; MT, methyltransferase.

production of a red cercosporinlike compound. To characterize this red metabolite, mycelia from both *C. fioriniae* strains were extracted with ethyl acetate. Reverse-phase HPLC analysis of extracts of both strains revealed a peak with a retention time and UV-Vis spectrum consistent with cercosporin in both extracts (Fig. 7 *A* and *B*). The presence of cercosporin was confirmed by ultra-performance LC (UPLC) electrospray ionization (ESI)-MS (Fig. 7*C*). Moreover, complementary resequencing of both isolates on the Illumina platform followed by automated genome assembly and gene prediction confirmed the presence of a *CTB* cluster in both genomes (*SI Appendix*, Fig. S11 and Table S8).

To assess whether *C. fioriniae* produces cercosporin during apple infection, apples were inoculated with the pathogen, and tissue samples were collected every other day from 1 to 14 d postinoculation. Regardless of time point or extraction methodology, we were unable to detect cercosporin from infected apple. However, by infiltrating apples with defined amounts of cercosporin, we determined that the isolation efficiency is ∼5% (*SI Appendix*, Figs. S12 and S13). Consequently, any cercosporin produced by *C. fioriniae* during infection is likely rapidly bound or modified by apple tissue such that its recovery by extraction is poor and below our level of detection by HPLC or ESI-MS. To provide additional support for the involvement of cercosporin in *C. fioriniae* infection, we infiltrated cercosporin into apple fruit and visually compared the phenotype of the infiltrated area to *C. fioriniae*-infected apple. At 5 d postinfiltration/inoculation, cercosporin-infiltrated apple exhibited similar symptomology as *C. fioriniae*-infected apple (*SI Appendix*, Fig. S14). We also quantified expression of *CTB1* using qRT-PCR since it is highly expressed during cercosporin biosynthesis and is the first committed step in the pathway (21). In concordance with earlier results where no cercosporin was detected from cultures grown in vitro in the absence of TSA, we likewise did not detect *CTB1* expression from this source (*SI Appendix*, Fig. S15). However, *CTB1* was found to be induced ∼11.9-fold in in vitro cultures with TSA and 2.5-fold in apple samples harvested 14 d postinoculation (*SI Appendix*, Fig. S15). Because amplification products were designed to span introns, amplicons were sequenced and verified to be derived from cDNA.

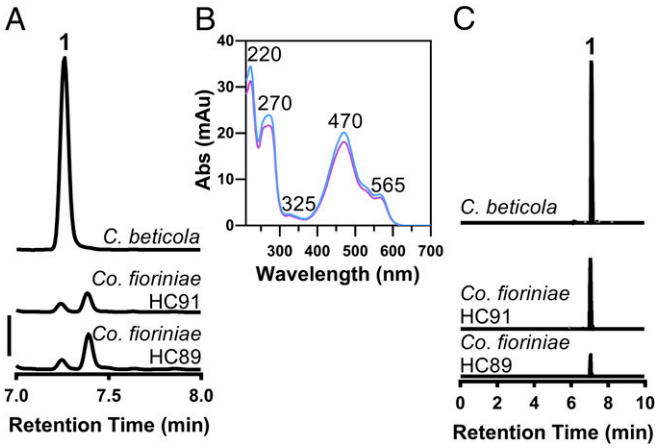

Fig. 7. HPLC and UPLC-ESI-MS analysis of *C. fioriniae* strains. (*A*) HPLC chromatograms at 280 nm of wild-type *C. beticola* and *C. fioriniae* strains HC89 and HC91. (Scale bar, 100 mAu.) (*B*) UV-Vis spectra of cercosporin (7.25-min retention time) extracted from *C. fioriniae* HC89 (shown in blue) and HC91 (in purple). Wavelengths of relevant UV maxima are indicated. (*C*) Extracted-ion chromatograms (*m/z* 535.1604) obtained by UPLC-ESI-MS, demonstrating cercosporin production in *C. beticola* and *C. fioriniae* HC89 and HC91.

We also attempted to isolate cercosporin from *C. higginsianum*-infected *Arabidopsis* leaves, since previous studies indicated the distinct induction of this cluster from *in planta* appressoria [22 h postinoculation (hpi)] and the biotrophic phase of infection (40 hpi) but indicated repression during in vitro growth and the necrotrophic phase of infection (60 hpi) (43). Again, we were unable to detect cercosporin from infected *Arabidopsis* leaves regardless of the extraction methodology or time point after inoculation. Given the relatively low amount of fungal biomass associated with the early time points when the *CTB* cluster is induced during *Arabidopsis* infection, we hypothesize that the amount of cercosporin produced *in planta* is below our current limits of detection.

Discussion

Several hypotheses exist for the maintenance of SM biosynthetic genes as clusters. In one, unlinked SM pathway genes are at a greater risk for dissociation during meiotic recombination (52) or chromosomal rearrangements (53). Additionally, clustering may facilitate strict coordination of gene expression, which may be particularly important during the biosynthesis of SMs that have potentially toxic or chemically unstable intermediates to ensure their efficient conversion to final end products (54). Horizontal transfer and maintenance of the *CTB* cluster specifically among plant pathogens suggests that it was critical for disease development in diverse pathosystems, including rice blast caused by *M. oryzae* and various anthracnose diseases caused by *Colletotrichum* spp. on many different crops. The *CTB* clusters in *C. higginsianum* and *C. graminicola* were reported as one of the few SM clusters between these species that are microsyntenic (43). Moreover, O'Connell et al. (43) detected specific up-regulation of the *CTB* cluster in *C. higginsianum* during colonization of *Arabidopsis*. Indeed, 9 of 14 *C. higginsianum CTB* genes were among the top 100 most highly expressed genes *in planta*. Recent analysis of natural selection processes in *C. graminicola* identified orthologs of *CTB* genes *CTB1* and *CFP* among the ∼80 genes undergoing significant positive selection (55), further suggesting a role in pathogenicity. Interestingly, the *CTB* clusters of *Colletotrichum* spp. and *M. oryzae* contain additional genes: two short-chain dehydrogenases, an additional desaturase, a ferric-chelate reductase, and an NmrA-like family protein, which has been reported (56) to act as negative transcriptional regulator.

The identification of cercosporin production in two isolates of *C. fioriniae* may have significant implications for the apple packing, storage, and processing industries. Bitter rot, caused by *Colletotrichum* spp., is one of the top pre- and postharvest pathogens of apple (57). This disease is a major problem for the apple industry because it limits fresh fruit in the field and during storage and has a quiescent stage, allowing decay to occur on seemingly high-quality apples, only to come out of storage rotten (57, 58). Hence, contamination of processed apple products with cercosporin could be a significant health hazard. For example, other fungal-produced toxins (e.g., patulin, citrinin, and penicillic acid) can contaminate processed apple products (59). Patulin, produced by *Penicillium* spp., is the most troubling because it is carcinogenic; consequently, the United States and Europe have strict patulin limits in fruit juices and processed pome-fruit products (59, 60). It may be necessary to will focus on the role of cercosporin production during the *Colletotrichum*-apple fruit interactions in addition to assaying processed fruit products made from apples with bitter rot symptoms to determine levels of the toxin in fruit. Although only *C. fioriniae* and *C. higginsianum* strains were analyzed for the ability to produce cercosporin, the identification of highly similar *CTB* clusters in other *Colletotrichum* spp. (*SI Appendix*, Figs. S10 and S11 and Table S8) suggests that cercosporin production may be widespread in this genus. Future studies directed toward analysis of *CTB* cluster expression among various *C. fioriniae* isolates and apple

cultivars will be necessary to confirm whether cercosporin is necessary for virulence of this pathogen.

The microsynteny outside the established *CTB* cluster prompted us to test whether the flanking genes in *C. beticola* are also required for cercosporin biosynthesis. Notably, we observed that these flanking genes, similar to the established *CTB* genes, were up-regulated under cercosporin-inducing conditions. Furthermore, targeted gene replacement of *CTB9*, *CTB10*, *CTB11*, and *CTB12* completely abolished cercosporin biosynthesis, while replacement of *CTB9* and *CTB10* resulted in the accumulation of a red metabolite, defined here as precercosporin. We thus conclude that the *CTB* cluster is significantly larger than previously described (19).

The isolation and characterization of an intermediate in the cercosporin biosynthetic pathway (precercosporin) strongly suggests that formation of the unique seven-membered methylenedioxy bridge in the final product is the result of a two-step process requiring three genes. First, one of two precursor aryl methoxyl groups of *ent* (+)-calphostin D (Fig. 6) is removed, followed by oxidative ring closure by CTB9, an apparent α-ketoglutarate–dependent dioxygenase, in collaboration with CTB10. The precise role of CTB10, a putative dehydratase, in ring closure is unclear, but it could serve to facilitate closure of the unfavorable seven-membered methylenedioxy ring. In contrast, a single cytochrome P450 is known to convert two aryl *ortho*-methoxyl groups into the relatively more common five-membered methylenedioxy group in alkaloid biosynthesis (61). We attribute the single demethylation to an oxidative process possibly carried out by the flavin-dependent enzymes CTB5 or CTB7. CTB6 correlates to the SDR NAD(P)H-binding superfamily of oxidoreductases and could install the side-chain hydroxyl groups stereospecifically. Owing to the extreme instability of most pathway intermediates and the role feedback inhibition in response to these metabolites could play, our experience dictates that analysis of pathway knockouts alone will not lead to the full determination of cercosporin biosynthesis. Biochemical evaluation of the individual enzymes, as has been done with CTB3 (21) with synthetic substrates and product standards, will be necessary to accomplish this task.

A tentative cercosporin biosynthesis scheme was recently proposed (21) without knowledge of the expanded *CTB* cluster. However, in light of the identification of precercosporin and the potential functions of the other *CTB* genes, the previously proposed biosynthetic pathway (21) will have to be revised. While these investigations will be reported in due course, we suspect the fasciclin/laccase pair (CTB11/12) may act early in the pathway to dimerize the product of CTB3 (21) to the first perylenequinone intermediate, which would have precedent in synthetic chemistry (62) and in simpler laccase-mediated aryl–aryl dimerizations (35, 63, 64) (Fig. 6). CTB1 is an iterative, nonreducing PKS whose product is *nor*-toralactone (20). CTB3 is a bifunctional enzyme (an *O*-methyltransferase and FAD-dependent monooxygenase) that carries out sequential *O*-methylation in the presence of *S*-adenosylmethionine and oxidative decarboxylation to cercoquinone C (21). We hypothesize that intermediate steps of *O*-dimethylation and side-chain ketone reduction, in unspecified order, are mediated by CTB2 and potentially CTB6, respectively, as noted above.

Despite sustained research on cercosporin for several decades, there are significant knowledge gaps in cercosporin biosynthesis. Our data have shed light on cercosporin biology and will have significant impact on cercosporin research in particular and on perylenequinone research in general. The finding that at least one species in the important plant pathogenic genus *Colletotrichum* can produce cercosporin has significant implications for disease management. Moreover, since *C. fioriniae* may secrete cercosporin into apple food products that may be directly consumed by humans, the toxic effects of cercosporin on human health may need to be considered.

Materials and Methods

For further information, see *SI Appendix, SI Materials and Methods* and figshare under DOI: 10.6084/m9.figshare.4056522. Custom code is permanently archived at Zenodo under DOI: 10.5281/zenodo.1156551.

Fungal genomic DNA was isolated from mycelia scraped from the surface of agar Petri plates. Library preparations and sequencing on the Illumina platform was performed by BGI Americas Corp. For *C. beticola*, three genomic libraries with increasing insert size (500 bp, 5 Kbp, and 10 Kbp) were sequenced. For *C. berteroae*, *C. nicotianae*, and *C. fioriniae* strains HC89 and HC91, single, short insert libraries (500 bp) were sequenced. For *C. beticola* specifically, optical maps were prepared using the Argus (OpGen) and BioNano Genomics platforms and subsequently used to scaffold contigs into large supercontigs. A combination of ab initio gene prediction, homologous protein alignment, and transcript alignment followed by extensive manual curation was used to prepare draft gene models for *C. beticola*. *C. beticola*-trained Augustus parameters were used for automated protein-coding gene modeling in the case of *C. berteroae*, *C. canescens*, and *C. nicotianae*. Genome assemblies and annotations, if applicable, are deposited in the NCBI GenBank database and listed under BioProject PRJA270309. Accession numbers for *C. beticola*, *C. berteroae*, *C. nicotianae*, and *C. fioriniae* strains HC89 and HC91 are LKMD00000000, PNEN00000000, POSS00000000, and PNFH00000000, and PNFI00000000, respectively.

Mycelial plugs of wild-type and mutant *C. beticola* were placed on top of eight "thin" PDA (Difco) plates (3.0 mL of PDA per 50-mm Petri plate). Cultures were incubated at 22 °C for 1 wk under continuous light. PDA and mycelia were ground under liquid nitrogen and lyophilized to dryness twice. The resulting powder was resuspended in water acidified with HCl (pH <1), allowed to sit 10 min, and filtered. The filtrate was extracted thrice with ethyl acetate. These extracts were pooled, washed with brine, and evaporated to dryness. The extracted metabolites were resuspended in 500 μL of methanol and analyzed by HPLC on an Agilent 1200 fitted with a Kinetex XB-C18 column (4.6 × 75 mm, 2.6 μm; Phenomenex). Injections of 1 μL were run at 1.25 mL/min with a linear gradient of 5% A/95% B to 95% A/5% B over 10.8 min, where solvent A was acetonitrile + 0.1% formic acid and solvent B was 0.1% formic acid. Chromatograms were monitored at 436, 280, and 210 nm, and UV-Vis spectra were recorded over a range of 210 to 800 nm. High-resolution mass data were obtained from a Waters Acquity/Xevo-G2 UPLC-ESI-MS in positive-ion mode.

ACKNOWLEDGMENTS. We thank W. Underwood and T. L. Friesen [US Department of Agriculture (USDA) Agricultural Research Service (ARS)] for review of the manuscript, A. G. Newman for helpful discussions and a reference sample of cercosporin, and N. Metz (USDA–ARS) for excellent technical assistance. Prof. M. Muller and L. Fürtges (University of Freiburg) are thanked for discussion of fungal laccases and unpublished results. This project was supported by a Long-Term Fellowship of the European Molecular Biology Organization (ALTF 359-2013) and a postdoctoral fellowship of the Research Foundation Flanders (FWO 12B8116N) (to R.d.J.); the USDA-ARS Current Research Information System Project 3060-22000-049 (to M.D.B.); National Institutes of Health Grants R01 ES001670 (to C.A.T.) and T32 GM080189 (to C.R.H.-R.); and Netherlands Organization for Scientific Research Grant 833.13.007 (to M.K.E.). Mention of trade names or commercial products in this publication is solely for the purpose of providing specific information and does not imply recommendation or endorsement by the USDA.

1. Groenewald M, Groenewald JZ, Braun U, Crous PW (2006) Host range of *Cercospora apii* and *C. beticola* and description of *C. apiicola*, a novel species from celery. *Mycologia* 98:275–285.
2. Fuckel K (1863) Fungi *Rhenani exsiccati*, Fasc. I–IV. *Hedwigia* 2:132–136.
3. Secor GA, Rivera VV, Khan MFR, Gudmestad NC (2010) Monitoring fungicide sensitivity of *Cercospora beticola* of sugar beet for disease management decisions. *Plant Dis* 94:1272–1282.
4. Wrather A, et al. (2010) Effect of diseases on soybean yield in the top eight producing countries in 2006. *Plant Health Prog* 10:1094.
5. Ward JMJ, Stromberg EL, Nowell DC, Nutter FW (1999) Gray leaf spot: A disease of global importance in maize production. *Plant Dis* 83:884–895.
6. Mani KK, Hollier CA, Groth DE (2017) Effect of cultivar susceptibility and planting date on narrow brown leaf spot progression in rice. *Crop Prot* 102:88–93.
7. Uppala S, Zhou XG (2018) Field efficacy of fungicides for management of sheath blight and narrow brown leaf spot of rice. *Crop Prot* 104:72–77.
8. Olatinwo RO, Prabha TV, Paz JO, Hoogenboom G (2012) Predicting favorable conditions for early leaf spot of peanut using output from the weather research and forecasting (WRF) model. *Int J Biometeorol* 56:259–268.

9. Stergiopoulos I, Collemare J, Mehrabi R, De Wit PJGM (2013) Phytotoxic secondary metabolites and peptides produced by plant pathogenic Dothideomycete fungi. *FEMS Microbiol Rev* 37:67–93.
10. Goodwin SB, Dunkle LD (2010) Cercosporin production in Cercospora and related anamorphs of Mycosphaerella. Cercospora *Leaf Spot of Sugar Beet and Related Species*, eds Lartey RT, Weiland JJ, Panella L, Crous PW, Windels CE (Am Phytopathol Soc, St. Paul), pp 97–108.
11. Daub ME, Ehrenshaft M (2000) The photoactivated *Cercospora* toxin cercosporin: Contributions to plant disease and fundamental biology. *Annu Rev Phytopathol* 38: 461–490.
12. Daub ME, Hangarter RP (1983) Light-induced production of singlet oxygen and superoxide by the fungal toxin, cercosporin. *Plant Physiol* 73:855–857.
13. Dobrowolski DC, Foote CS (1983) Cercosporin, a singlet oxygen generator. *Angew Chem Int Ed Engl* 22:720–721.
14. Daub ME (1982) Cercosporin, a photosensitizing toxin from *Cercospora* species. *Phytopathology* 72:370–374.
15. Gunasinghe N, You MP, Cawthray GR, Barbetti MJ (2016) Cercosporin from *Pseudocercosporella capsellae* and its critical role in white leaf spot development. *Plant Dis* 100:1521–1531.
16. Crous PW, et al. (2013) Phylogenetic lineages in *Pseudocercospora*. *Stud Mycol* 75: 37–114.
17. Daub ME (1981) Destruction of tobacco cell-membranes by the photosensitizing toxin, cercosporin. *Phytopathology* 71:869.
18. Daub ME (1987) Resistance of fungi to the photosensitizing toxin, cercosporin. *Phytopathology* 77:1515–1520.
19. Chen H, Lee MH, Daub ME, Chung KR (2007) Molecular analysis of the cercosporin biosynthetic gene cluster in *Cercospora nicotianae*. *Mol Microbiol* 64:755–770.
20. Newman AG, Vagstad AL, Belecki K, Scheerer JR, Townsend CA (2012) Analysis of the cercosporin polyketide synthase CTB1 reveals a new fungal thioesterase function. *Chem Commun (Camb)* 48:11772–11774.
21. Newman AG, Townsend CA (2016) Molecular characterization of the cercosporin biosynthetic pathway in the fungal plant pathogen *Cercospora nicotianae*. *J Am Chem Soc* 138:4219–4228.
22. Choquer M, Lee MH, Bau HJ, Chung KR (2007) Deletion of a MFS transporter-like gene in *Cercospora nicotianae* reduces cercosporin toxin accumulation and fungal virulence. *FEBS Lett* 581:489–494.
23. Callahan TM, Rose MS, Meade MJ, Ehrenshaft M, Upchurch RG (1999) CFP, the putative cercosporin transporter of *Cercospora kikuchii*, is required for wild type cercosporin production, resistance, and virulence on soybean. *Mol Plant Microbe Interact* 12:901–910.
24. Chand R, et al. (2015) Draft genome sequence of *Cercospora canescens*: A leaf spot causing pathogen. *Curr Sci* 109:2103–2110.
25. Blin K, et al. (2013) antiSMASH 2.0–A versatile platform for genome mining of secondary metabolite producers. *Nucleic Acids Res* 41:W204–W212.
26. Ohm RA, et al. (2012) Diverse lifestyles and strategies of plant pathogenesis encoded in the genomes of eighteen *Dothideomycetes* fungi. *PLoS Pathog* 8:e1003037.
27. Collemare J, et al. (2014) Secondary metabolism and biotrophic lifestyle in the tomato pathogen *Cladosporium fulvum*. *PLoS One* 9:e85877.
28. Medema MH, Cimermancic P, Sali A, Takano E, Fischbach MA (2014) A systematic computational analysis of biosynthetic gene cluster evolution: Lessons for engineering biosynthesis. *PLOS Comput Biol* 10:e1004016.
29. Chooi Y-H, Muria-Gonzalez MJ, Solomon PS (2014) A genome-wide survey of the secondary metabolite biosynthesis genes in the wheat pathogen *Parastagonospora nodorum*. *Mycology* 5:192–206.
30. Koczyk G, Dawidziuk A, Popiel D (2015) The distant siblings—A phylogenomic roadmap illuminates the origins of extant diversity in fungal aromatic polyketide biosynthesis. *Genome Biol Evol* 7:3132–3154.
31. Stolzer M, et al. (2012) Inferring duplications, losses, transfers and incomplete lineage sorting with nonbinary species trees. *Bioinformatics* 28:i409–i415.
32. Tudzynski B, et al. (2003) Characterization of the final two genes of the gibberellin biosynthesis gene cluster of *Gibberella fujikuroi*: *Des* and *P450-3* encode GA4 desaturase and the 13-hydroxylase, respectively. *J Biol Chem* 278:28635–28643.
33. Kim J-E, et al. (2005) Putative polyketide synthase and laccase genes for biosynthesis of aurofusarin in *Gibberella zeae*. *Appl Environ Microbiol* 71:1701–1708.
34. Williams JS, Thomas M, Clarke DJ (2005) The gene *stlA* encodes a phenylalanine ammonia-lyase that is involved in the production of a stilbene antibiotic in *Photorhabdus luminescens* TT01. *Microbiology* 151:2543–2550.
35. Frandsen RJN, et al. (2011) Two novel classes of enzymes are required for the biosynthesis of aurofusarin in *Fusarium graminearum*. *J Biol Chem* 286:10419–10428.
36. Gao Q, et al. (2011) Genome sequencing and comparative transcriptomics of the model entomopathogenic fungi *Metarhizium anisopliae* and *M. acridum*. *PLoS Genet* 7:e1001264.
37. Shimodaira H (2002) An approximately unbiased test of phylogenetic tree selection. *Syst Biol* 51:492–508.
38. Shimodaira H, Hasegawa M (2001) CONSEL: For assessing the confidence of phylogenetic tree selection. *Bioinformatics* 17:1246–1247.
39. Wisecaver JH, Rokas A (2015) Fungal metabolic gene clusters—caravans traveling across genomes and environments. *Front Microbiol* 6:161.
40. Velho AC, Stadnik MJ, Casanova L, Mondino P, Alaniz S (2013) First report of *Colletotrichum nymphaeae* causing apple bitter rot in southern Brazil. *Plant Dis* 98:567.
41. Víchová J, Vejražka K, Cholastová T, Pokorný R, Hrudová E (2010) *Colletotrichum simmondsii* causing anthracnose on safflower in the Czech Republic. *Plant Dis* 95:79.
42. Cannon PF, Damm U, Johnston PR, Weir BS (2012) *Colletotrichum*–Current status and future directions. *Stud Mycol* 73:181–213.
43. O'Connell RJ, et al. (2012) Lifestyle transitions in plant pathogenic *Colletotrichum fungi* deciphered by genome and transcriptome analyses. *Nat Genet* 44:1060–1065.
44. Sukno SA, García VM, Shaw BD, Thon MR (2008) Root infection and systemic colonization of maize by *Colletotrichum graminicola*. *Appl Environ Microbiol* 74:823–832.
45. Weir BS, Johnston PR, Damm U (2012) The *Colletotrichum gloeosporioides* species complex. *Stud Mycol* 73:115–180.
46. Damm U, et al. (2013) The *Colletotrichum orbiculare* species complex: Important pathogens of field crops and weeds. *Fungal Divers* 61:29–59.
47. Damm U, Cannon PF, Woudenberg JHC, Crous PW (2012) The *Colletotrichum acutatum* species complex. *Stud Mycol* 73:37–113.
48. Kasson MT, Pollok JR, Benhase EB, Jelesko JG (2014) First report of seedling blight of eastern poison ivy (*Toxicodendron radicans*) by *Colletotrichum fioriniae* in Virginia. *Plant Dis* 98:995.
49. Choquer M, et al. (2005) The *CTB1* gene encoding a fungal polyketide synthase is required for cercosporin biosynthesis and fungal virulence of *Cercospora nicotianae*. *Mol Plant Microbe Interact* 18:468–476.
50. Shwab EK, et al. (2007) Histone deacetylase activity regulates chemical diversity in *Aspergillus*. *Eukaryot Cell* 6:1656–1664.
51. Williams RB, Henrikson JC, Hoover AR, Lee AE, Cichewicz RH (2008) Epigenetic remodeling of the fungal secondary metabolome. *Org Biomol Chem* 6:1895–1897.
52. Galazka JM, Freitag M (2014) Variability of chromosome structure in pathogenic fungi–of 'ends and odds'. *Curr Opin Microbiol* 20:19–26.
53. de Jonge R, et al. (2013) Extensive chromosomal reshuffling drives evolution of virulence in an asexual pathogen. *Genome Res* 23:1271–1282.
54. McGary KL, Slot JC, Rokas A (2013) Physical linkage of metabolic genes in fungi is an adaptation against the accumulation of toxic intermediate compounds. *Proc Natl Acad Sci USA* 110:11481–11486.
55. Rech GE, Sanz-Martín JM, Anisimova M, Sukno SA, Thon MR (2014) Natural selection on coding and noncoding DNA sequences is associated with virulence genes in a plant pathogenic fungus. *Genome Biol Evol* 6:2368–2379.
56. Stammers DK, et al. (2001) The structure of the negative transcriptional regulator NmrA reveals a structural superfamily which includes the short-chain dehydrogenase/reductases. *EMBO J* 20:6619–6626.
57. Munir M, Amsden B, Dixon E, Vaillancourt L, Gauthier NAW (2016) Characterization of *Colletotrichum* species causing bitter rot of apple in Kentucky orchards. *Plant Dis* 100:2194–2203.
58. Kou LP, Gaskins V, Luo YG, Jurick WM (2013) First report of Colletotrichum fioriniae causing postharvest decay on 'Nittany' apple fruit in the United States. *Plant Dis* 98: 993.
59. Wright SAI (2015) Patulin in food. *Curr Opin Food Sci* 5:105–109.
60. Puel O, Galtier P, Oswald IP (2010) Biosynthesis and toxicological effects of patulin. *Toxins (Basel)* 2:613–631.
61. Díaz Chávez ML, Rolf M, Gesell A, Kutchan TM (2011) Characterization of two methylenedioxy bridge-forming cytochrome P450-dependent enzymes of alkaloid formation in the Mexican prickly poppy *Argemone mexicana*. *Arch Biochem Biophys* 507:186–193.
62. Hauser FM, Sengupta D, Corlett SA (1994) Optically active total synthesis of calphostin D. *J Org Chem* 59:1967–1969.
63. Bode SE, Drochner D, Müller M (2007) Synthesis, biosynthesis, and absolute configuration of vioxanthin. *Angew Chem Int Ed Engl* 46:5916–5920.
64. Kawaguchi M, et al. (2018) Discovery of a fungal multicopper oxidase that catalyzes the regioselective coupling of a tricyclic naphthopyranone to produce atropisomers. *Angew Chem Int Ed Engl* 57:5115–5119.